

1997

Design of a one-liter autoclave flow process

Frank Orozco
San Jose State University

Follow this and additional works at: https://scholarworks.sjsu.edu/etd_theses

Recommended Citation

Orozco, Frank, "Design of a one-liter autoclave flow process" (1997). *Master's Theses*. 1461.
DOI: <https://doi.org/10.31979/etd.8ftb-hy9g>
https://scholarworks.sjsu.edu/etd_theses/1461

This Thesis is brought to you for free and open access by the Master's Theses and Graduate Research at SJSU ScholarWorks. It has been accepted for inclusion in Master's Theses by an authorized administrator of SJSU ScholarWorks. For more information, please contact scholarworks@sjsu.edu.

INFORMATION TO USERS

This manuscript has been reproduced from the microfilm master. UMI films the text directly from the original or copy submitted. Thus, some thesis and dissertation copies are in typewriter face, while others may be from any type of computer printer.

The quality of this reproduction is dependent upon the quality of the copy submitted. Broken or indistinct print, colored or poor quality illustrations and photographs, print bleedthrough, substandard margins, and improper alignment can adversely affect reproduction.

In the unlikely event that the author did not send UMI a complete manuscript and there are missing pages, these will be noted. Also, if unauthorized copyright material had to be removed, a note will indicate the deletion.

Oversize materials (e.g., maps, drawings, charts) are reproduced by sectioning the original, beginning at the upper left-hand corner and continuing from left to right in equal sections with small overlaps. Each original is also photographed in one exposure and is included in reduced form at the back of the book.

Photographs included in the original manuscript have been reproduced xerographically in this copy. Higher quality 6" x 9" black and white photographic prints are available for any photographs or illustrations appearing in this copy for an additional charge. Contact UMI directly to order.

UMI

A Bell & Howell Information Company
300 North Zeeb Road, Ann Arbor MI 48106-1346 USA
313/761-4700 800/521-0600

DESIGN OF A ONE-LITER AUTOCLAVE FLOW PROCESS

A Thesis
Presented to
The Faculty of the Department of
Chemical Engineering
San Jose State University

In Partial Fulfillment
of the Requirements for the Degree
Master of Science

by
Frank Orozco
May 1997

UMI Number: 1384710

UMI Microform 1384710
Copyright 1997, by UMI Company. All rights reserved.

**This microform edition is protected against unauthorized
copying under Title 17, United States Code.**

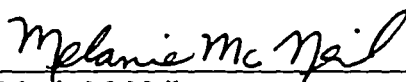
UMI
300 North Zeeb Road
Ann Arbor, MI 48103

© 1997

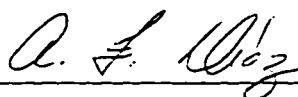
Frank Orozco

ALL RIGHTS RESERVED

APPROVED FOR THE DEPARTMENT OF CHEMICAL ENGINEERING



Dr. Melanie McNeil

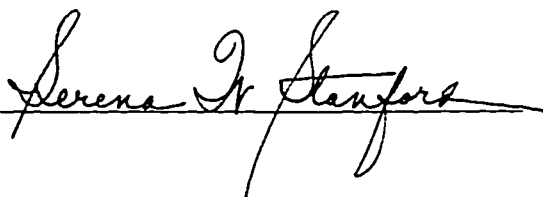


Dr. Art Diaz



Dr. Peter Millet, EPRI

APPROVED FOR THE UNIVERSITY



ABSTRACT

DESIGN OF A ONE-LITER AUTOCLAVE FLOW PROCESS

by Frank Orozco

An experimental one-liter autoclave system that simulates the tube-tube support crevice in the steam generators of nuclear power plants has been designed and tested. The system includes data acquisition software, instrumentation for process variables measurement, and all necessary equipment for fluid moving and heating. The system was proven to operate in blow-down mode (liquid in all lines) under reaction conditions indicating that the autoclave is nearly full and that steady-state operation is attainable in the absence of crevice boiling. An experiment using a 120 ppm sodium chloride solution and a carbon-packed tube-tube support crevice proved that salt accumulation will occur once the crevice is installed. Thus, it has been shown that crevice hide-out is the only possibility for accumulation of species within the autoclave under the range of conditions studied.

ACKNOWLEDGMENTS

The author would like to thank Dr. Melanie McNeil and Dr. Peter Millet for the suggestions they offered throughout this work, Paul Rogers for the brainstorming sessions and for helping with the day-to-day operation. I would also like to thank my wife for the love and support, and the Lord for giving me the strength to reach this day. This work is dedicated to my family, who always believed in me.

TABLE OF CONTENTS

ABSTRACT	iv
ACKNOWLEDGMENTS	v
TABLE OF CONTENTS	vi
LIST OF FIGURES	vii
LIST OF TABLES	ix
CHAPTER 1. INTRODUCTION AND BACKGROUND	1
CHAPTER 2. REVIEW OF PREVIOUS WORK	5
CHAPTER 3. MATERIALS AND METHODS	15
3.1 Research Objectives	15
3.2 Process Design	16
3.3 Conductivity Measurements	21
3.4 Data Acquisition (DAQ)	26
3.5 Non-Crevice Experimental Procedure	31
3.6 Packed-Crevice Experimental Procedure	32
CHAPTER 4. RESULTS AND PROCEDURES	33
4.1 Material Balance	33
4.2 Hideout-Hideout Return	37
CHAPTER 5. CONCLUSIONS AND RECOMMENDATIONS	42
NOMENCLATURE	45
REFERENCES	47

LIST OF FIGURES

Figure 1. Pressurized Water Reactor (PWR) power plant.	2
Figure 2. Steam generator tube and tube support.	3
Figure 3. Weight of NaCl in crevice.	10
Figure 4. Typical surge in outlet concentration after switching off the crevice heater.	12
Figure 5. Influence of calcium, magnesium and silica containing precipitates on crevice pH(t) as a function of the molar ratio.	13
Figure 6. Inconel 600 autoclave dimensions.	16
Figure 7. Central tube heater with crevice positioned around eight radially positioned thermocouples.	18
Figure 8. Process flow diagram.	19
Figure 9. Ion chromatograph block diagram.	21
Figure 10. Conductivity cell calibration curve for 0.3 to 3 parts per million NaCl samples.	23
Figure 11. Conductivity cell calibration curve for 3 to 25 parts per million NaCl samples.	23
Figure 12. Conductivity cell calibration curve for 32 to 150 parts per million NaCl samples.	24
Figure 13. Ion chromatograph calibration curve for 0.3 to 3 parts per million NaCl samples.	24

Figure 14. Ion chromatograph calibration curve for 3 to 25 parts per million NaCl samples.	25
Figure 15. Ion chromatograph calibration curve for 32 to 150 parts per million NaCl samples.	25
Figure 16. Data acquisition hardware	27
Figure 17. Pressure transducer voltage to pressure conversion.	30
Figure 18. Effluent NaCl concentration over time for the non-cage experiment at 400 psia.	34
Figure 19. Effluent NaCl Mass Flow Rate for packed crevice experiment.	39

LIST OF TABLES

Table 1. Model equations.	7
Table 2. Boundary conditions.	7
Table 3. Operating conditions for non-crevice experiments.	31

CHAPTER 1. INTRODUCTION AND BACKGROUND

A major goal of the nuclear power industry is to minimize corrosion within the steam generating circuits of nuclear power plants. It is estimated that corrosion is costing the nuclear power industry half a billion dollars per year world-wide. Hence, for decades, researchers have been investigating ways to minimize corrosion. Some attempts have included changing the materials of construction, removing the causes of the corrosion from the feedwater before introducing it into the system, and introducing additives to change the chemistry. Some of the attempts have worked, some have not, and many are still under investigation.

Corrosion products increase operating and maintenance costs for several reasons. For example, the fouling of the heat transfer surfaces of the Pressurized Water Reactor (PWR) decreases the overall thermal efficiency of a plant. Even more costly to the industry is the shut down of a unit for maintenance. Not only is there monetary loss due to the temporary shut down of the unit, but the plant must also pay for the replacement power that must be supplied. The most costly consequence of corrosion, however, is the replacement of the parts, or the entire unit. The Steam Generator (SG) of a PWR is highly susceptible to corrosion. It was designed to operate for forty years, but many have been decommissioned after only ten years of operation.

The Steam Generator is found downstream from the main pressure vessel where the nuclear reaction is taking place. Figure 1 is a representation of a Pressurized Water Reactor Nuclear Plant.

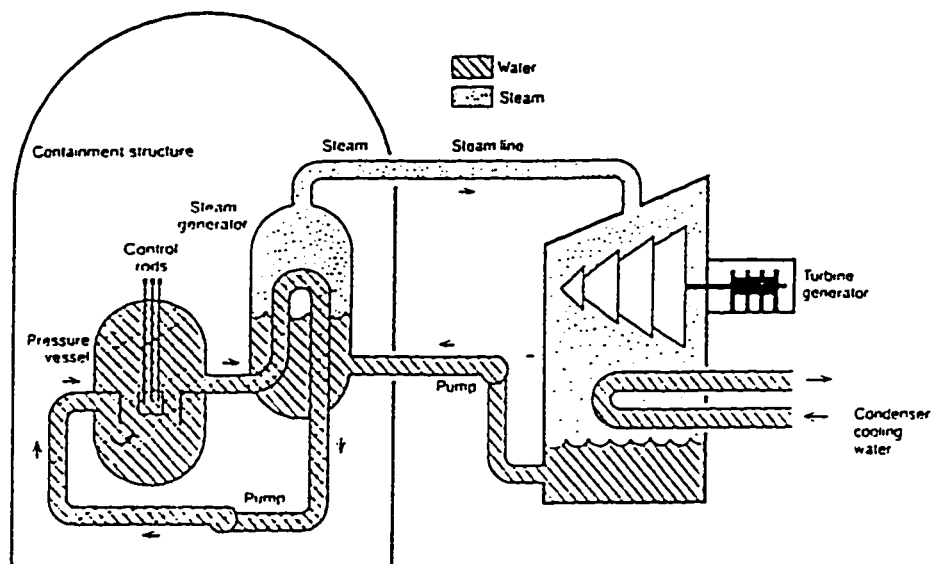


Figure 1. Pressurized Water Reactor (PWR) power plant.

The uranium fuel is contained within fuel rods that are immersed in water in the pressure vessel. The heat generated by the nuclear fission chain reaction is transferred to the water, but because the vessel is at a pressure of 2250 psia, the water does not evaporate when it is heated to 620°F. This water is instead pumped through the tube side of the SG where it will transfer its heat to generate steam.

The SG is essentially a shell-and-tube heat exchanger. The hot water flows in the interior of mill annealed alloy 600 tubes and transfers its heat to the water on the shell side. Because the shell side pressure is only 880 psia, the water is boiled and steam is produced. This steam is sent to a turbine where the shaft is connected to an electrical generator.

Several different corrosion products have been found locally in SG's. Their precise identification has been made possible as analytical techniques became more sophisticated. Researchers have determined that corrosion solids contain many cationic

and anionic species that are found in soluble form in the feedwater. Examples of such species include calcium, nickel, sodium, magnesium, sulfates, chlorides, and most importantly, iron.

The composition of the steam generator water phase is of most concern relative to corrosion. The concentration of additives or impurities can range from parts per billion to the weight percent level at different points in the cycle. Impurities in pressurized water reactors tend to concentrate in flow starved regions of the steam generator where crevices are formed between the steam generator tubing and the support structures.

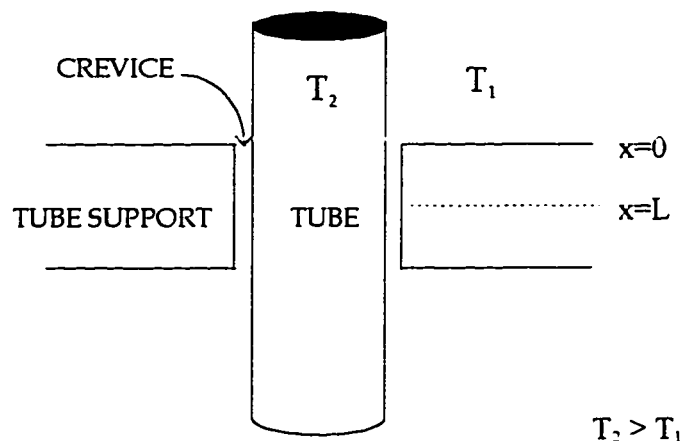


Figure 2. Steam generator tube and tube support.

The impurities concentrate in the flow starved region for two main reasons: 1) the impurities are non-volatile and 2) water is volatile. Therefore, as the water is boiled off, the impurities are being concentrated within the crevice volume. This concentration process can be taken to such an extent that the salt ions, caustics, and acids found in the crevice will enhance the corrosion process. Researchers have thus investigated controlling the chemistry in the crevices. However, in order to control the crevice chemistry, a

method must be developed to either monitor the crevice chemistry on a real-time basis or predict its composition from other measured parameters. Monitoring the crevice directly is not easily accomplished. An alternative approach is to simulate the crevice in a small-scale device and monitor the “hideout return” (HOR) of impurities when the process is shut down. When the power level is decreased, the impurities tend to diffuse into the bulk water where they can be sampled.

CHAPTER 2. REVIEW OF PREVIOUS WORK

Problems of Steam Generator corrosion in the nuclear industry have evolved in a sequential manner. Early problems were solved, but with these solutions, new problems emerged. Some of the major early problems the nuclear industry faced included tube wastage, a generalized tube thinning, and tube denting, which resulted from the corrosion buildup on the carbon steel tube supports. These problems were remedied and are not an issue in today's pressurized water reactor steam generators (Douglas, 1995).

Today, the biggest concern related to corrosion in tube-tube support crevices is intergranular corrosion, in which the chemical attack tends to follow the grain boundaries in the tube metal. In the absence of significant stress, the grain boundaries degrade more or less uniformly, beginning at the surface resulting in a form of deterioration called intergranular attack (IGA). If the metal has relatively higher stresses remaining from fabrication or generated by operation, cracks may propagate into the tube metal along grain boundaries, a phenomenon known as intergranular stress corrosion cracking (IGSCC) (Douglas, 1995).

The Electric Power Research Institute has developed water chemistry guidelines to minimize IGA/SCC. Several computer tools have also been developed to help utilities select and implement the appropriate water chemistry program. These tools are used in conjunction with the water chemistry guidelines to perform specific analyses to support the development of hideout return, MRC, and pH control programs.

Molar Ratio Control (MRC) is a methodology for reducing the growth rates of IGA/SCC. The practice of MRC is based on the assumption that the crevice pH influences crack initiation and growth and can be modified by controlling the ratio of strong acid anions and strong basic cations in the steam generator bulk water. By developing an understanding of the relationship between the bulk water chemistry and the crevice chemistry, appropriate changes can be made to the bulk water to proactively control the crevice chemistry.

Molar Ratio Control has now been adopted at nearly 50 percent of U.S. PWR's with older SG designs. MRC is achieved by adding ammonium chloride at a low level to the steam generator. An upper limit for the SG chloride concentration under normal operation has been established as 5 parts per billion (ppb). MRC has also been used in Japan for some time. To date, no firm conclusions can be drawn as to the effectiveness of MRC in reducing IGSCC in U.S. plants.

It is believed that intergranular attack can be curtailed by creating a less corrosive environment in the crevice between the tubing and the tube support. Creating this environment has not been a simple task, and monitoring the crevice directly has proven difficult as well. Several different models have been developed that attempt to predict the environment in this crevice.

Millet and Fenton (1991) presented a mathematical model based on momentum, heat, and mass conservation laws for transport processes. The detailed development of the model can be found in Millet's Ph.D. dissertation (1991). The model describes the concentration process in fouled crevices and was intended to be used to predict the

concentration of a given species in the crevice solution as a function of time and at steady-state. The boundary conditions that are required to solve the equations can be found in Table 2, and their points of application can be seen in Figure 2. The crevice is considered symmetrical, so the equations are solved for only one half of the crevice, and it is assumed that the conditions are mirrored on the other half.

Table 1. Model equations.

(Millet and Fenton, 1991)

Conservation of Mass:	Two-Phase Flow Equations:
(1) $-\varepsilon \frac{\partial p}{\partial t} = \frac{\partial(\rho_l v_l)}{\partial x} + \frac{\partial(\rho_v v_v)}{\partial x}$	(5) $v_l = -\frac{k_l}{\mu_l} \left(\frac{\partial p_l}{\partial x} - \rho_l g \right)$
(2) $\rho_m = S \rho_l + (1-S) \rho_v$	(6) $v_v = -\frac{k_v}{\mu_v} \left(\frac{\partial p_v}{\partial x} - \rho_v g \right)$
Conservation of Energy:	(7) $k_l = k S_e^m$
(3) $\frac{2\pi H r_{sg}}{A_c} (T_p - T_s) = \frac{\partial(\rho_l v_l h_{fg})}{\partial x}$	(8) $k_v = k(1-S_e)^n$
Conservation of Species A:	(9) $S_e = \frac{S - S_r}{1 - S_r}$
(4) $\varepsilon \frac{\partial(Cs)}{\partial t} + \frac{\partial(cv_l)(1-k_{v-l})}{\partial x} = \frac{\partial \left[D_{es} \frac{\partial C}{\partial x} \right]}{\partial x}$	(10) $P_c = \rho_v - \rho_l = f[s]$
	(11) $T_s = T_{so} + 6.5c$

Table 2. Boundary conditions.

(Millet and Fenton, 1991)

@ $x = 0$:	$C = C_o$ $\rho_l = \rho_o$ $P_l = P_v = P_o$ $P_c = 0$ $S_e = S_r$
@ $x = L$:	$\frac{\partial C}{\partial x} = 0$ $v_l = v_v = 0$

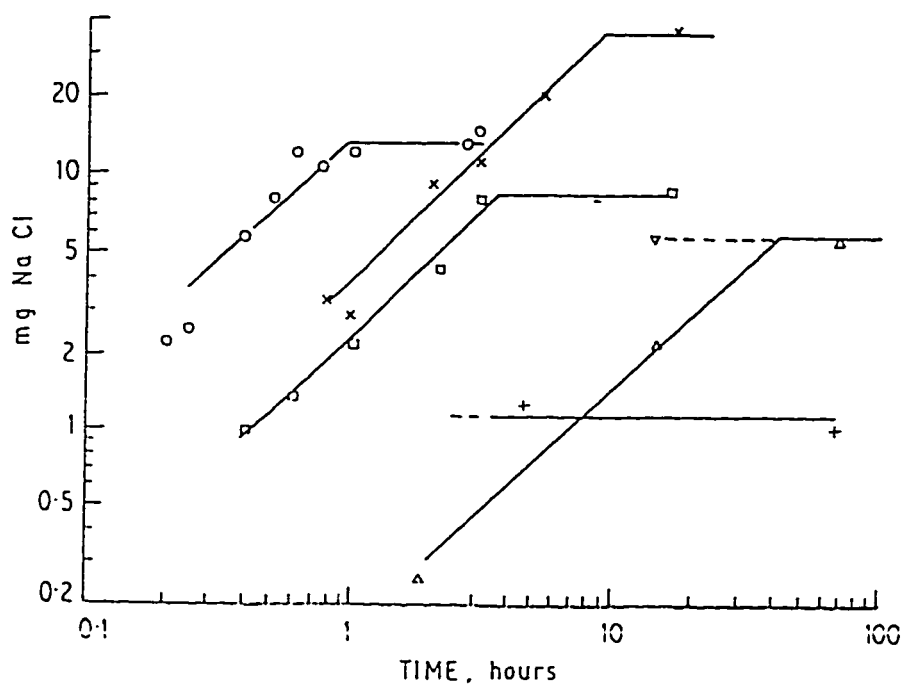
Boiling heat transfer within the wetted length is described by a single nucleate boiling heat transfer coefficient. Heat transferred from the steam blanketed region is considered negligible compared to the nucleate boiling flux. The pore solution temperature is approximated by the saturation temperature of the crevice pore.

Salt concentration in the crevices is a main contributor to the corrosion of the steam generator tubing. Mann and Castle (1987) studied salt hideout in the support plate crevices of a 1-liter pressure vessel. Their setup simulated the large-scale unit in many ways. The pressure vessel was operated at the same temperature and pressure as the full-scale unit. They simulated the hot tube-side water with a cartridge heater. The heater could be operated at the same temperature as the tube-side water without the risk of radiation exposure. The crevice was packed with carbon fiber to simulate the corrosion solids that accumulate in the crevices. The shell-side water was evaporated and the salt ions were concentrated in the crevice.

The objective of their work was to define crevice hideout and return processes in order to assist the formulation of water chemistry guidelines for minimizing the occurrence of tube and support structure corrosion. The work was done using sodium chloride at different feed concentrations and different cartridge heater heat fluxes. The advantage of their work is that they only had to worry about one crevice, as opposed to thousands; they did not have to worry about radiation exposure; and they could easily shut the process down to perform the “hideout” return experiments.

Two key predictions were made by Millet's model and supported by Mann and Castle's experimental work. First, the maximum concentration in the crevice is independent of the bulk water concentration; an asymptotic limit is reached regardless of the bulk water concentration. Secondly, as the crevice solution is being concentrated, its boiling point is being elevated. A maximum concentration limit is reached when the boiling temperature of the concentrated solution is equal to the temperature of the hot fluid within the steam generator tube. At this point, there is no more boiling of the shell-side fluid, and thus, no further concentration of the impurities in the crevice. When this condition has been achieved, it is said that the crevice has reached its thermodynamic limit. Therefore, it seems that the concentration in the crevice is really a function of the degree of superheat. The degree of superheat is the temperature difference between the inner tube T_1 and the initial saturation temperature of the bulk liquid T_2 . The location of these temperatures is shown in Figure 2. If the temperature of the tube-side fluid where increased, further concentration of impurities could resume. This result is illustrated in Figure 3, which shows crevice concentrations over time for different feed concentrations and heat fluxes.

The transient model was used to predict accumulation rates. The concentration profile first becomes thermodynamically limited deep within the crevice. As time proceeds, the concentration increases to the thermodynamic limit based on the available superheat throughout the crevice. It has been observed experimentally and confirmed with the model that the rate of accumulation is nearly linear to the bulk water concentration and also directly proportional to the superheat. This result can also be seen in Figure 3.



	FEED CONCENTRATION	HEATER POWER	
	mg/kg NaCl	Watts	Blu/ft ² hr
0	120	150	47,000
X	12	230	72,000
□	12	150	47,000
+	12	85	27,000
△	1.2	150	47,000
▽	1.2	150	47,000

THE POINT MARKED ▽ WAS MEASURED AFTER PREVIOUSLY ESTABLISHING EQUILIBRIUM AT 120 mg/kg NaCl, 150 WATTS.

Figure 3. Weight of NaCl in crevice.
(Mann & Castle, 1987)

Engineers at EPRI have proposed two methods for predicting crevice chemistry (Millet, 1995). The first consists of measuring the bulk water impurities on a real time

basis, and through empirical measurements, assessing the rate at which the bulk water impurities are concentrating in the crevices. This rate is then integrated over time to yield the crevice inventory, from which the crevice pH can be directly calculated. This approach is complicated by the fact that the rate of concentration is not only a function of crevice chemistry, but is also a function of the physical condition of the steam generator crevices. Parameters such as porosity, permeability, and tortuosity of the pores within the solid corrosion products have an affect on the concentration process. Many of these variables change frequently enough that frequent measurement of concentration efficiency may be required to improve this technique as a method for predicting crevice chemistry.

“Hideout” return chemistry when the plant is shut down is another possible method. When the heat flux is reduced, the concentrated solutions tend to diffuse out of the crevice and into the bulk. This result is illustrated in Figure 4, where a surge in effluent concentration is observed upon shutdown. The curve flattens out over time as all of the impurities have diffused from the crevice.

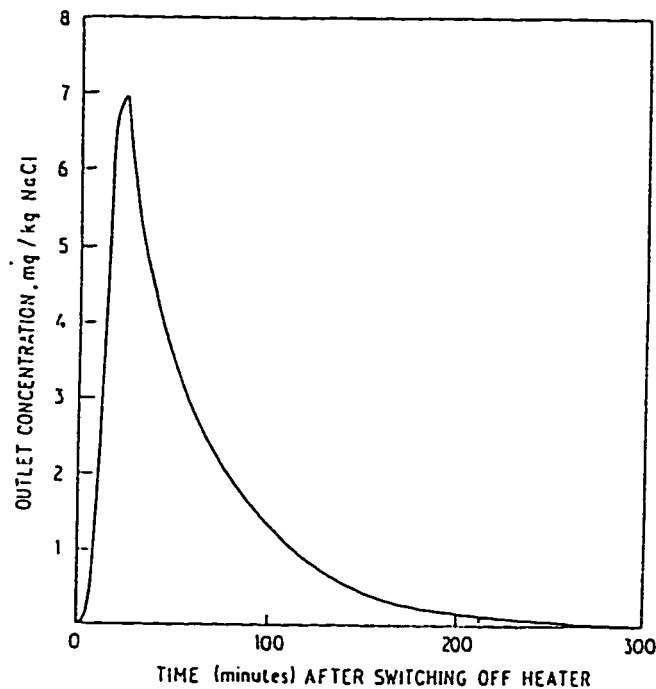


Figure 4. Typical surge in outlet concentration after switching off the crevice heater.
(Mann & Castle, 1987)

The two major limitations of this technique are (1) only an average crevice chemistry across the thousands of crevices can be inferred, and (2) this technique can only be applied when a plant is shut down; which is once per year at most.

A molar ratio indicator (MRI) is defined using hideout return data. It is based on the relative ratio of ionic impurities that are believed to be returning from the crevice solution during hideout return. It is thought that attempts to modify the crevice solution to produce an MRI as close as possible to unity gives a higher probability of achieving a crevice pH within the target range for minimizing localized corrosion.

$$MRI = \frac{(Na + K)}{(Cl + excessSO_4)} \quad (12)$$

A number of individual studies indicate that maintaining a crevice high temperature pH(t) in the range 5-9 should minimize IGSCC of mill annealed alloy 600 steam generator tubing. It is thought that the crevice pH(t) will be within the target range if the ratio of the highly soluble cation and anion impurities in the crevice is near one, and if sufficient quantities of less soluble impurities are present. Other impurities such as magnesium, silicon, and calcium in the crevice serve as pH buffers.

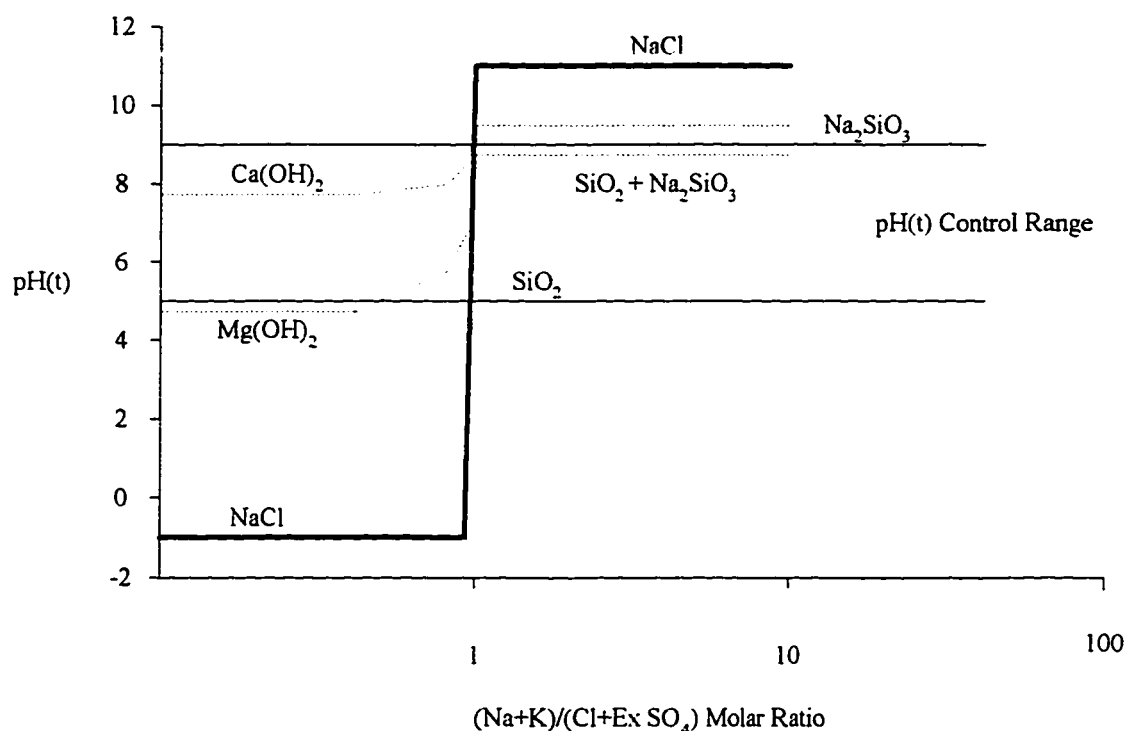


Figure 5. Influence of calcium, magnesium and silica containing precipitates on crevice pH(t) as a function of the molar ratio.
(Millet, Brobst & Riddle, 1993)

The curve labeled NaCl in Figure 5 shows the results of titrating NaCl with HCl or NaOH in the absence of any other species. It is apparent the NaCl solutions have no buffering capacity so that the pH goes very acidic at Na/Cl ratios only slightly less than 1 and extremely caustic at ratios slightly greater than 1. In the absence of other crevice impurities it would be very difficult if not impossible to control the crevice pH in the target pH range of 5-9 to minimize intergranular stress corrosion cracking (IGSCC).

A second approach for evaluating HOR chemistry assumes the cumulative hideout return data can be described by two basic models: (1) a linear model described by hideout return rate being relatively constant, and (2) an exponential release described by a rate constant. Some plant HOR data show that when release occurs, the integrated return show an exponential increase. This type of release can be viewed as being controlled by a rate constant.

CHAPTER 3. MATERIALS AND METHODS

The design of a flow process that can be used to simulate the corrosion process in steam generators is the focus of this work. The chosen design allows the operation of the system at flow rates that seem to be the standard range of operation for the crevice corrosion studies to be performed in the future.

3.1 Research Objectives

- 1) Design the layout of an experimental system and confirm the operability of the data analysis equipment, and data acquisition software.
- 2) Test steady-state operation in absence of crevice.
- 3.) Verify accumulation when packed crevice is present.

The two passive heaters, along with a single active heater, are Cole-Parmer model MBH-6015900T band type heaters. They are all situated around the exterior of the autoclave. These heaters are connected to on/off controllers. The two passive heaters operate at full power. Presently, each heater is wired to give a maximum power output of 180 watts. Both can be re-wired to supply a maximum output of 450 watts. They serve to heat the system near the setpoint, but not quite attain it. The active heater is used to fine tune the temperature. It is connected to a thermocouple which reads the autoclave's external wall temperature. This heater is plugged into a variac and is capable of supplying up to 450 watts of power. Power will only be supplied to this heater when the passive heaters are on.

The ceramic fiber insulated autoclave has a 1-liter capacity when empty. Approximately 25% of water is displaced with the introduction of the central tube heater and the cage that forms the crevice. A 250-volt cartridge heater is located within an eight inch long, 3/4 inch O.D. tube. The heater sits in a 54.3 wt% KNO_3 , 45.7 wt% NaNO_3 eutectic salt mixture. The specific mixture was selected because of its excellent heat transfer characteristics. Eight 1/16 inch thermocouples are also spot welded to the internal surface of the tube. As shown in Figure 7, these thermocouples are radially positioned at different levels so that temperature distributions can be detected within the crevice. It is believed that this arrangement will help attempts to understand the concentration process that occurs within the crevice.

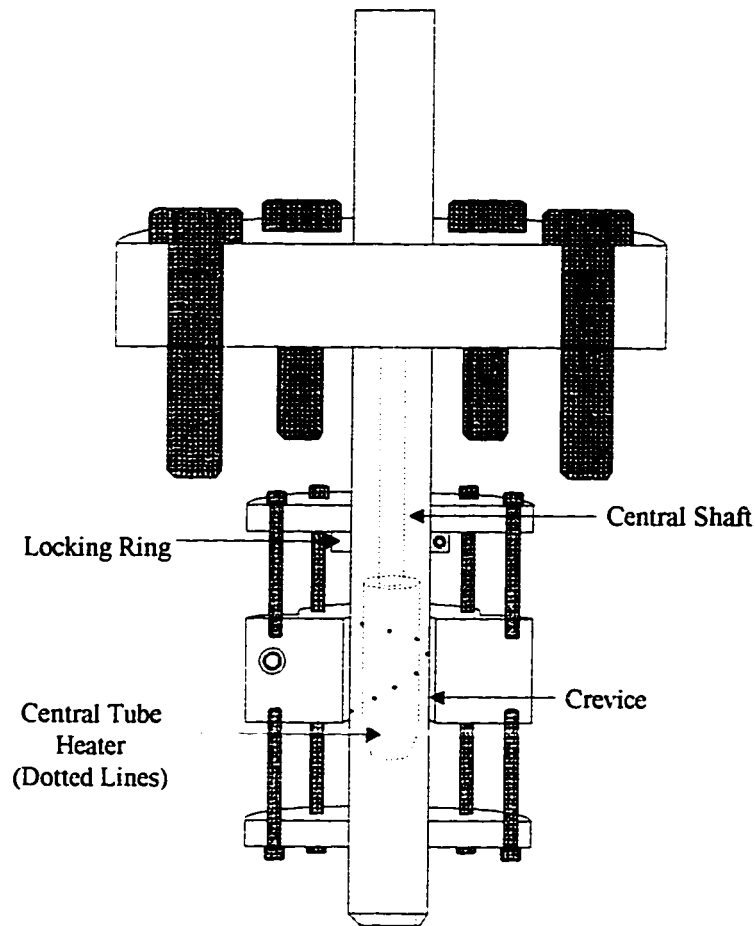


Figure 7. Central tube heater with crevice positioned around eight radially positioned thermocouples.

The cage that forms the crevice is positioned around the tube so that the crevice is at the level of the eight thermocouples. The cage is a “clamshell” type (named due to its resemblance to a clam shell). Above and below the crevice are two flanges that help secure the crevice in its intended position on the tube. Teflon O-rings found within these flanges seal any crevices that may have been possible between the flanges and the tube. The upper and lower flanges are connected to the clam shell by four 3-inch pins. The separation between the flanges and the clam shell is two inches. An additional locking ring

was to be positioned under the cage so that it would not move during operation. Unfortunately, the available tube will not allow the locking ring to fit under the cage. Instead, the locking ring will be placed below the top flange, as shown in Figure 7. This will make it a bit more difficult to remove the crevice for analysis, but the task is manageable.

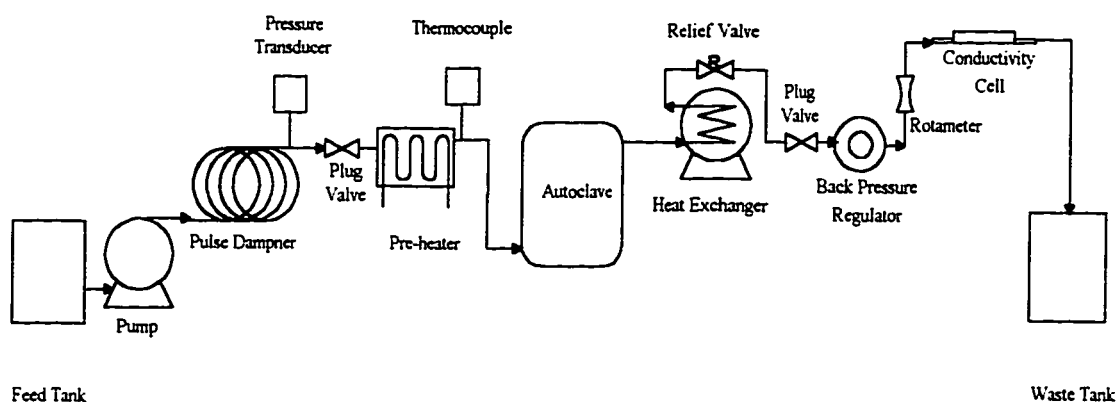


Figure 8. Process flow diagram.

The overall process flow diagram is shown in Figure 8. Water is pumped from the ten gallon feed tank with a Pulsar 25H diaphragm metering pump. This pump was selected because of its ease and flexibility of operation. It does, however, produce a substantial hammer with each stroke. A pulse dampener purchased from Altech was installed along with approximately seven feet of coiled 1/16-inch Teflon tubing. This setup virtually eliminates the pulsing effects from the pump. The tubing system selected was 1/4 inch O.D. 316 stainless steel with twenty-five thousandths of an inch wall thickness. Connections are made with Swagelock fittings. A pressure transducer followed by a preheater are connected upstream from the autoclave. The transducer

outputs a current signal that is converted to a voltage via parallel resistors. This signal is sent to the data acquisition system. A thermocouple measures the preheat temperature before the water enters the autoclave. The preheat water temperature should be just a few degrees below saturation. It has been determined that approximately 540 watts of power are required to obtain conditions just below saturation at 880 psia.

The autoclave system should operate at equilibrium. The rate of steam formation should equal the rate of condensation in the autoclave. The steam formed should be minimal, and should not extend to the level of the autoclave outlet. These conditions ensure that the salt concentration in the autoclave is equal to that of the feed.

The outlet from the autoclave flows into a heat exchanger which reduces the temperature to 25°C. A pressure relief valve is also installed to prevent over pressurizing the system and causing damage to the equipment. Its cracking pressure has been set to 1200 psia and has been tested for reliability. Finally, an in-line conductivity cell measures the solution conductivity. It must be horizontally positioned to ensure complete wetting of the platinum sensor to obtain proper readings. Effluent samples can also be sampled periodically and analyzed with an ion chromatograph.

The system pressure is set with a Grove model number 155 back-pressure regulator (BPR). This BPR was difficult to find because the flow rate is so low and the pressure is so great. The original BPR was not able to control the system pressure and purging would result. The Grove meets the system requirements and has made a significant difference in obtaining and maintaining system conditions. The BPR creates the back-pressure with a spring that is internally mounted. The system pressure is easily

altered with a turn of the dial. A rotameter is also found at the outlet for convenient flow measurement.

3.3 Conductivity Measurements

The ion chromatograph was utilized in the salt hide out experiments. Figure 9 is a block diagram representation of the unit being utilized in this research.

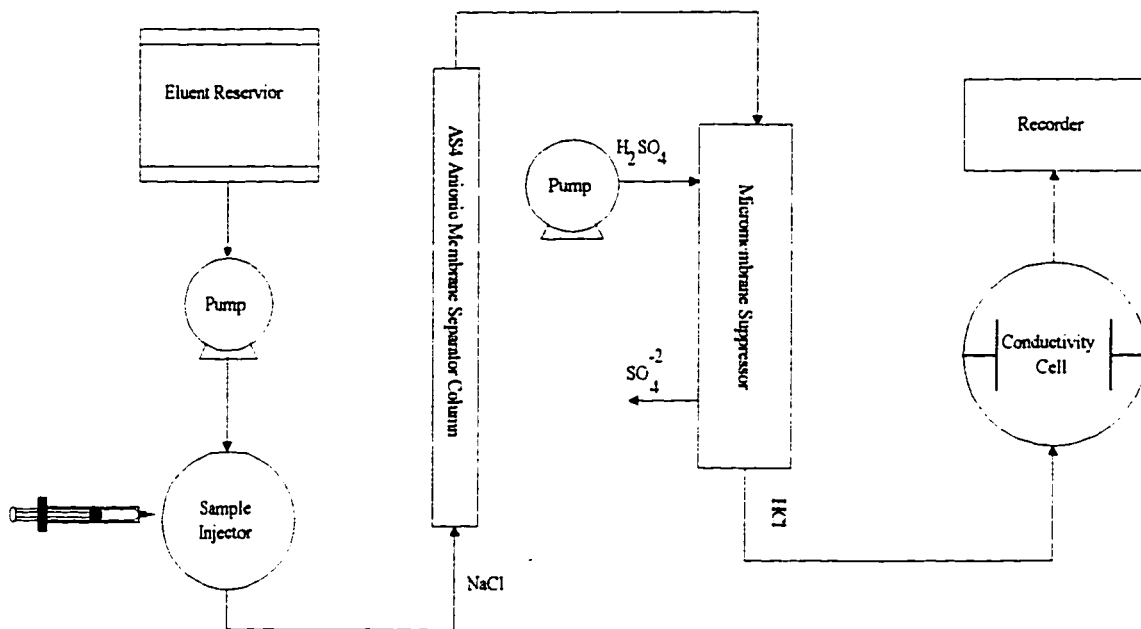


Figure 9. Ion chromatograph block diagram.

The unit is equipped with a anionic membrane separator, a micromembrane suppresser, an ion detector, and regenerant and eluent pumps. The anionic membrane separator retains the cationic species while allowing all anionic species to pass to the micromembrane suppresser. The regenerant, sulfuric acid, serves to amplify the signal for greater accuracy. It does so through a displacement reaction between sulfuric acid and the

anionic species in the sample. The reaction product is hydrochloric acid, a strong acid, which is highly dissociative. This dissociative nature allows better conductivity measurement of the chloride anion.

In-line conductivity measurements were taken using a Cole-Parmer model number H01481-65 conductivity cell. The feed was measured with dip cell model number H01481-64 before it was pumped into the system. Each cell consists of a platinum drive plate which receives a sine wave signal voltage. This voltage forces a current through the solution to a sense plate in the cell where it is converted back to a voltage and finally to a digital readout. These cells are extremely sensitive and must be used properly to obtain accurate results.

Three calibration curves have been constructed for three different orders of magnitude for both the ion chromatograph and the conductivity meters. The first calibration curve is for species in the 0.3 and 3 ppm range, the second for 3 and 25 ppm, and the third for 25 and 150 ppm. The calibration curves are shown in Figures 10-15.

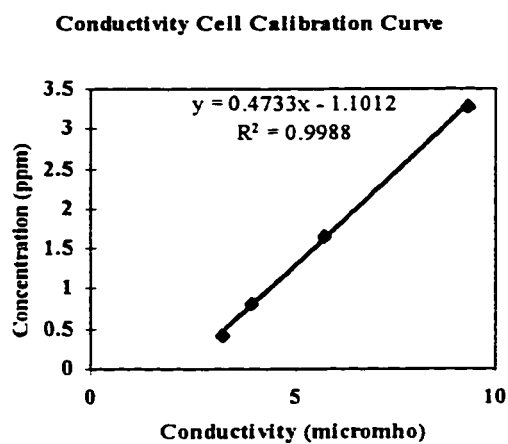


Figure 10. Conductivity cell calibration curve for 0.3 to 3 parts per million NaCl samples.

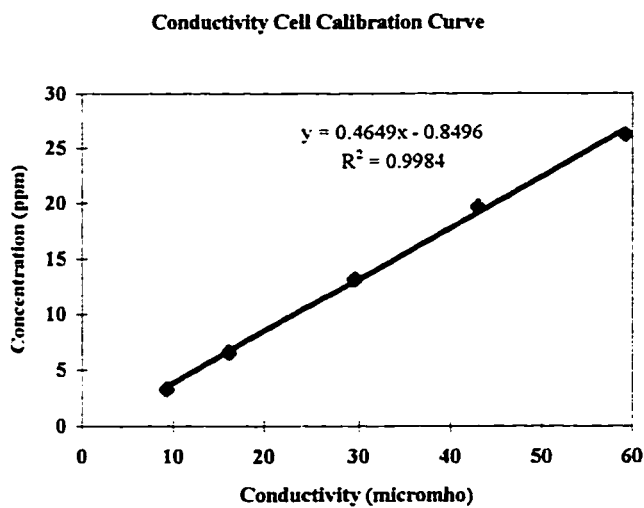


Figure 11. Conductivity cell calibration curve for 3 to 25 parts per million NaCl samples.

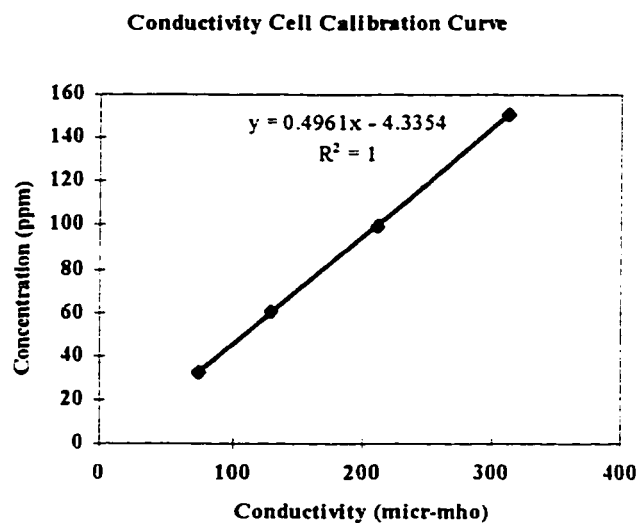


Figure 12. Conductivity cell calibration curve for 32 to 150 parts per million NaCl samples.

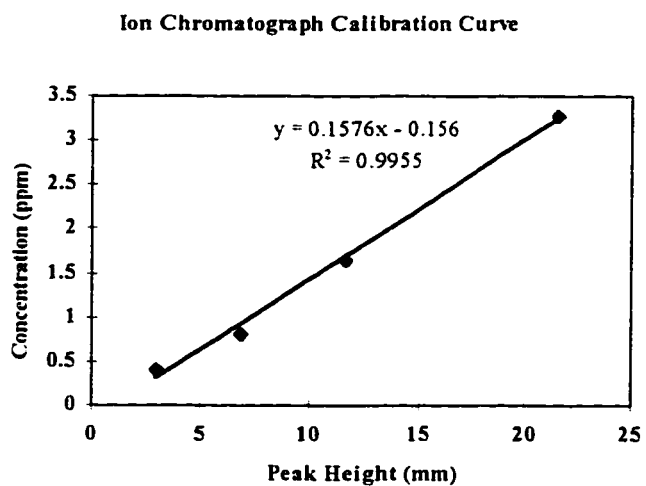


Figure 13. Ion chromatograph calibration curve for 0.3 to 3 parts per million NaCl samples.

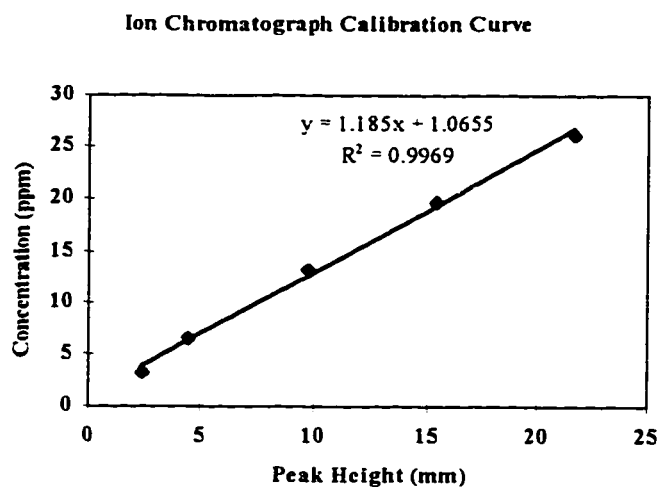


Figure 14. Ion chromatograph calibration curve for 3 to 25 parts per million NaCl samples.

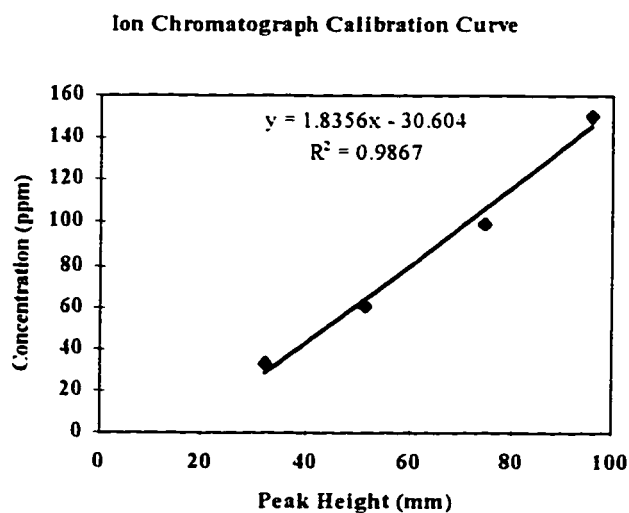


Figure 15. Ion chromatograph calibration curve for 32 to 150 parts per million NaCl samples.

Best fit lines have been drawn through the data points. The equation of the best fit line has been included along with the correlation coefficient. The data appears to be linear and

at worst, 98.7% (corresponding to R^2 of Figure 15) of the variability in the samples would be accounted for by the best fit lines.

3.4 Data Acquisition (DAQ)

To properly configure the data acquisition system, it is necessary to understand the system it will be monitoring and the level of the signals that will be sent. The autoclave flow process will be monitored for temperature at approximately ten different points in the process, pressure measurements will be taken by a single pressure transducer, and a conductivity measurement will also be taken. The typical temperature-voltage signal will be approximately 30mV and will never exceed 50mV. The pressure and conductivity signals will be slightly higher, but will never exceed 2 volts.

LabView data acquisition software/hardware has been selected for this purpose. Figure 16 is a schematic representation of the hardware that will be discussed in the following section. The hardware consists of an AT-MIO-16 data acquisition (DAQ) board, an SCXI-1000 chassis equipped with two signal amplifying/conditioning modules operating in multiplexed mode. Multiplexing allows data acquisition of several channels on multiple modules by continuously scanning the channels and acquiring the data. To minimize the possibility of noise interference of the smaller signals, the higher level voltages were separated from the lower level voltages by connecting them on separate terminal blocks. Therefore, all thermocouple signals going to the DAQ board are sent through terminal block 1300 which is connected to the SCXI-1100 module. Pressure and

on-line conductivity measurements are sent through terminal block-1320 which is connected to the SCXI-1120 module.

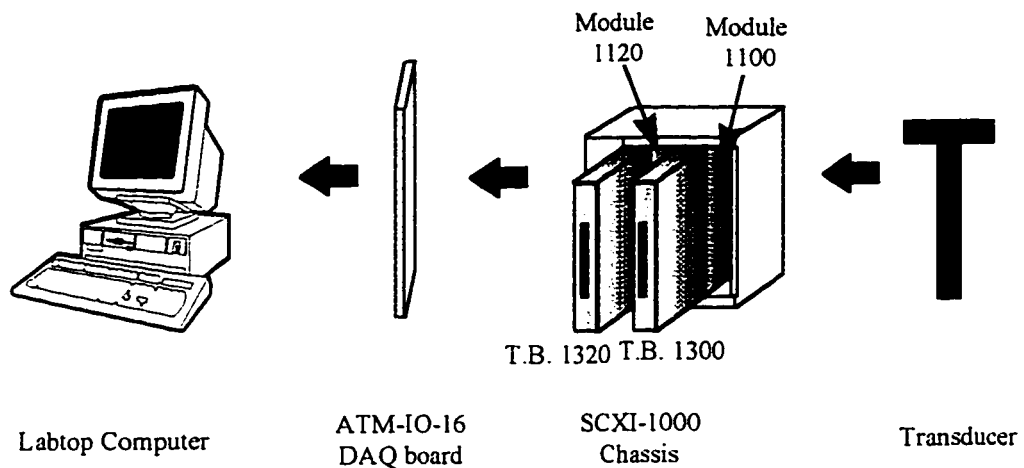


Figure 16. Data acquisition hardware

The hardware and software must be properly configured in order to obtain accurate readings. Hardware configuration changes are done via jumper settings and software changes are made in the NIDAQ Configuration Utility. There are several items that must be properly set which are worth mentioning at this time.

The most important piece of hardware for the DAQ system is the DAQ board. This board is plugged directly into the computer's main board and communicates with the chassis via a ribbon cable. Configuration of this board must be done on both the hardware and the software. For this system that will never see a voltage signal over two volts, it is recommended that the analog input/output be set to bipolar mode ($\pm 5V$). This setting will give better sensitivity, and thus more accurate measurements. Also, the Differential (DIFF) input mode should be used. DIFF input means that each input signal has its own

reference, and the difference between each signal and its reference is measured. This mode is recommended for the autoclave process because it eliminates grounding problems that could result with such low-level input signals.

Module-1100 receives temperature signals via terminal block 1300. Proper hardware configuration of module-1100 requires that jumper W10 be set in position A-R0-R1. This setting is used when in differential mode on a MIO data acquisition board. Jumpers W7 and W8 should be in position B, which connects unnecessary pins of the front connector to the analog ground, eliminating any unwanted noise from these pins. Finally, the thermocouples should be grounded to the chassis ground screw. This is done by connecting a wire from the negative screw terminal (CH-) to the chassis ground screw terminal. Since multiple channels were in use, the CH- were daisy chained to the chassis ground. Terminal block 1300 had one setting that required revision. The temperature sensor must be set to multiplexed mode (MTEMP). Setting jumper W1 to MTEMP connects the temperature sensor output to the SCXI-1100 output multiplexer, which now allows the DAQ board to scan the programmed channels on the module for voltage signals.

The thermocouple module also requires proper selection of software settings. Terminal block 1300 has cold junction compensation (CJC) that must be programmed to the proper address. This means that the reference point on the terminal block must be identified in the software so that proper temperature corrections can be made. Also, the “CJC” sensor used by this terminal block is an IC type, and K-type thermocouples have been used throughout the process. The signal input limits, found in the wiring diagram

must be properly set to apply the correct gain. The gain multiplies the signal by a constant to produce a higher output signal. A gain of 20 has been set in the wiring diagram as a result of setting the input limits to ± 0.5 . With a typical temperature voltage signal being 30mV, the output signal to the data acquisition board would become 0.6 volts.

The pressure, temperatures, and effluent conductivity are measured every 10 seconds by the data acquisition (the sampling rate can be set through the software); data is stored in a file that can later be opened using Excel. LabView comes with sub-programs which use polynomial expressions to convert between temperature and voltage for the specified thermocouple type. The pressure transducer produced a current signal with a bandwidth of 4-20 mA. Two 249 ohm resistor in parallel were used to convert this current to a voltage which could then be sent to terminal block 1320. The voltage signal range for the transducer is between 0.50 and 2.5 volts. Signal voltages of this magnitude do not need to be amplified and the gain should be set to one. Gain settings on module 1120 are set with jumpers on the board itself. Figure 17 illustrates the relationship that exists between this voltage and the pressure.

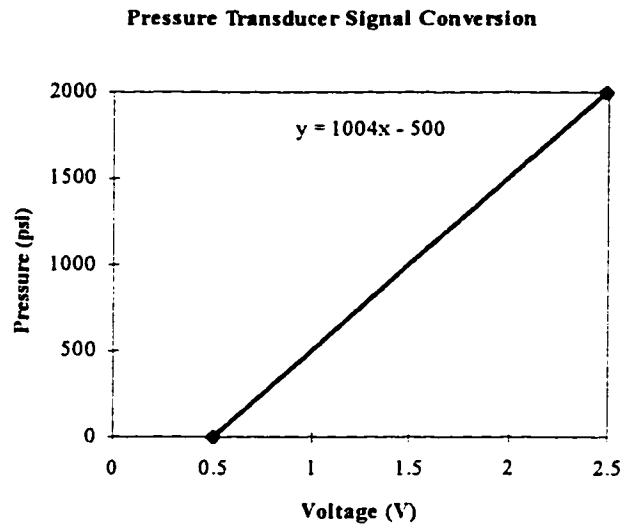


Figure 17. Pressure transducer voltage to pressure conversion.

The conductivity meter sends a voltage to the data acquisition which is exactly equal to the conductivity (micro-mho). No signal conversion was necessary and a connection between the meter and the terminal block was the only requirement.

Because there is a great deal of equipment involved in the operation of this process, proper grounding is essential. The autoclave has been grounded, and all electrical connections have been tested for proper grounding. The computer has been placed on a grounding pad, and the ribbon cable has been shielded with aluminum wrap. All thermocouples have been grounded within the terminal blocks as well. The typical thermocouple voltage reading for our system will be under 40 millivolts, and minimal amounts of noise will have a great affect on this small signal.

3.5 Non-Cage Experimental Procedure

The goal of this work is to provide an experimental flow process that can be used to simulate the corrosion process in steam generators used in the nuclear power industry. The system will be used in future crevice chemistry studies in which impurities from the feed water will accumulate in the crevice. Before any crevice experiments are run, however, it is necessary to confirm that there is no accumulation of species in the absence of the cage. These experiments are necessary to determine if species are actually hiding solely as a result of the cage during evaporation or whether there are other parts of the system where they can accumulate.

The following two experimental runs were performed to prove these ends:

Table 3. Operating conditions for non-cage experiments.

	<u>Experiment #1</u>	<u>Experiment #2</u>
Pressure (psia)	400	880
Feed temperature (°F)	442	525
Ramping rate (°F/hour)	92	92
Flow rate (mL/min.)	30	30
Feed concentration (ppm)	50	50

The pressure, temperature, and flow rate were variable during ramping. As the system vapor pressure increased and the density decreased, the flow rate was adjusted to compensate for the pressure and density changes of the system. Once the final conditions were attained, the system flow rate was set at 30 mL/min.

Conductivity measurements were taken to determine the effluent concentration throughout the experiment. The system was allowed to run an additional two hours once saturation was achieved.

3.6 Packed-Crevice Experimental Procedure

Another test necessary to demonstrate the operability of the system is to show that accumulation will indeed occur in a packed-crevice. Therefore, the crevice was randomly packed with 0.7 micron pitch-based carbon fibers. These fibers are chemically inert and will only affect the system from a physical standpoint. The cage was vertically positioned so that the crevice was at the level of the eight internal thermocouples and of the cartridge heater.

The system was fed a 120 mg/kg sodium chloride solution at a rate of 30 mL/min. The start-up procedures for this experiment were identical to the non-crevice experiment performed at 880 psia. Ramping occurred over a five hour period at a rate of 92°F per hour. The preheated water temperature was approximately five degrees under saturation. Once steady-state had been reached, the central heater was switched on at 230 Watts for one hour to allow salt-hideout in the crevice. The heater was then turned off to allow hide-out return from the crevice.

CHAPTER 4. RESULTS AND PROCEDURES

The following section consists of the results of the crevice/non-crevice tests. Two sets of runs were performed, one with and the other without the cage that forms the crevice. The purpose of the first experiments was to prove that salt would not accumulate without a crevice and the second proved that salt would accumulate in the presence of a packed crevice.

4.1 Material Balance

The non-cage experiments were carried out with a feed water NaCl concentration of 50 mg/kg and a flow rate of 30 mL/min. During ramping, however, the flow rate was variable to compensate for the increasing vapor pressure and the decreasing density of the water. The system was operated at two different saturation conditions. The first was performed at 400 psia and 445°F, and the second was at 880 psia and 530°F. The ramping time to attain these conditions is four and five hours, respectively, and ramping occurred at a rate of 92°F per hour. The pressure was initially set to half of the desired value, and then increased to 10 psi below final operating pressure at the start of the third hour of ramping. As the system temperature increased, the pressure rose to near the intended pressure; fine adjustments were then required to attain operating pressure. The final pre-heater temperature was five degrees below saturation. The active heaters supplied the

additional heat required to attain saturation conditions. The system was allowed to run an additional two hours once saturation conditions were attained.

The feed conductivity was measured prior to introduction into the system, and the outlet conductivity was continuously monitored with the flow cells. Samples were also taken for ion chromatography analysis every hour during ramping, and every 30 minutes while at saturation. With the aid of the conductivity measurements, a material balance showed no accumulation in the system in the absence of the cage. Figure 18 shows the outlet concentration over time for the non-cage experiment conducted at saturation conditions at a pressure of 880 psia.

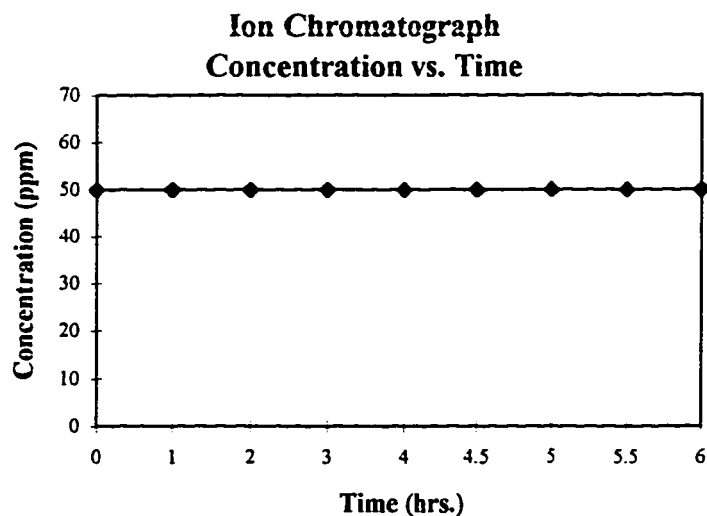


Figure 18. Effluent NaCl concentration over time for the non-cage experiment at 400 psia.

The initial data point is a measurement of the feedwater before introduction into the autoclave. Ramping occurred for the first three hours, and constant conditions were

maintained for an additional three hours. The concentration did not change which indicates that all ions entering the system are exiting. Because the flow during ramping was varied to compensate for pressure and density changes, it was possible to maintain a constant concentration. The fact that no accumulation was seen at any point in the run of the system in the absence of the cage proves that steady-state operation is attainable.

The material balance tests answer three key questions: (1) will salt accumulate in a cage-less autoclave? (2) is the water level above the crevice level?, and (3) is the water level above the outlet level?

The first question was answered by measuring the conductivity of the inlet and the outlet in non-cage experiments. Due to the smooth geometry of the autoclave and flow loop, there should be no preferential zone for hideout. Therefore, what enters the process should exit the process. If the conductivities are the same, there has been no accumulation, and it can be assumed that any accumulation in future experiments be the result of the inserted cage. Because of the sensitivity of the analytical instrumentation, it can be assumed that any hideout would have been detected in the non-cage experiments.

To properly simulate industrial units, it must be certain that the water level be above the crevice level. If this condition is not met, the heat transfer characteristics of the system would change because the thermal conductivity for saturated water is almost twenty times that of saturated steam at 530°F (SI units). Furthermore, the nucleate boiling regime that is most desirable in practical applications could not be attained. Instead, the crevice would be in a film boiling regime. The result would be a poor simulation of industrial units and a much reduced heat flux. Because the crevice is

positioned lower than the outlet, the answer to this question is most easily obtained through the answer to the third question.

The process should be in blow-down mode for proper operation. If the water level were not above the outlet level, the boiling process could be described similar to that which occurs in the crevice. The non-volatile species would accumulate in the autoclave while the water evaporates and exits the autoclave through the outlet. This steam line would later condense into a high purity water line because the non-volatile species have been left in the autoclave, and a drop in outlet conductivity would result. Figure 18 shows that this is not the case and that the system is indeed in blow-down mode. If the opposite were true, the liquid in the autoclave would be increasing in concentration. This liquid would begin to flow out once the salt concentration was high enough to elevate the solution boiling point and cause a decrease in the vaporization rate. The concentrated solution would also have an affect on the salt accumulation rate in crevice experiments because of the increased concentration driving force. The autoclave concentration would not only be impossible to determine, but it would be transient until the solution boiling point was elevated to a degree where the power supplied by the heaters could no longer sustain boiling.

It was discovered with the flow cells that the effluent conductivity was slightly higher than the inlet conductivity at higher operating temperatures. This was quite surprising since we believed that the conductivity could only decrease due to accumulation in the crevice. The in-line conductivity meter was consistently reading elevated values, therefore random error was probably not the cause of these variations. With the ion

chromatograph information showing no increase in anionic species, it is believed that the slight increase in conductivity is a result of cationic species being released through a corrosion process. Cationic species analysis was not performed, but visual inspection of the tubes would support this reasoning. There were a few instances when the tubing system developed a leak that appeared to be classic pitting corrosion. The holes that developed appeared as dark dots to the naked eye. Further inspection with an eye loop revealed that small holes existed through the tube wall. Pitting corrosion is a problem frequently encountered when running hot chloride solutions. Regular cleaning of the system will help the problem, but a more permanent solution would be replacing the tubing with a more corrosion resistant metal. The difference in conductivity as a result of this corrosion was no more than 1 ppm at the most severe operating conditions of 880 psia and 535°F.

4.2 Hideout-Hideout Return

The packed crevice experiment required the assembly of a carbon fiber-packed crevice between the tube and the tube support. The cage that forms the crevice was installed one section at a time (refer to Figure 7). The upper flange was inserted and measurements were taken to ensure that it was properly positioned. The locking ring was then inserted and tightly fastened to prevent the flange from sliding down. Next, carbon fibers were randomly positioned on one half of the clamshell that forms the crevice. This half was secured to the upper flange with two 3-inch screws. The assembly could now be

rotated so that the other clamshell half could be packed and inserted into the cage. The clamshell was screwed tight and the packed crevice was now in position with a porosity of approximately 0.5. The crevice porosity was determined by measuring the weight of the carbon fibers and using the density to determine the volume of carbon. The central tube and cage diameters were given in the autoclave schematics, so the crevice volume could be determined. The crevice porosity was then calculated as follows:

$$Porosity = 1 - \frac{Volume_{packing}}{Volume_{crevice}} \quad (13)$$

With the crevice securely in position, the lower flange could now be inserted and the cage assembly was complete.

Effluent samples were taken according to a set schedule during ramping and tube heating. Samples were taken for ion chromatograph analysis every hour during ramping, and every twenty minutes during crevice boiling. Sampling once the heat flux was removed occurred every two to five minutes. Hideout-return initially occurs at such a rapid rate that for a good profile, sampling is required frequently during the surge (first ten minutes after flux removal), but can be less frequent as the concentration drops off asymptotically.

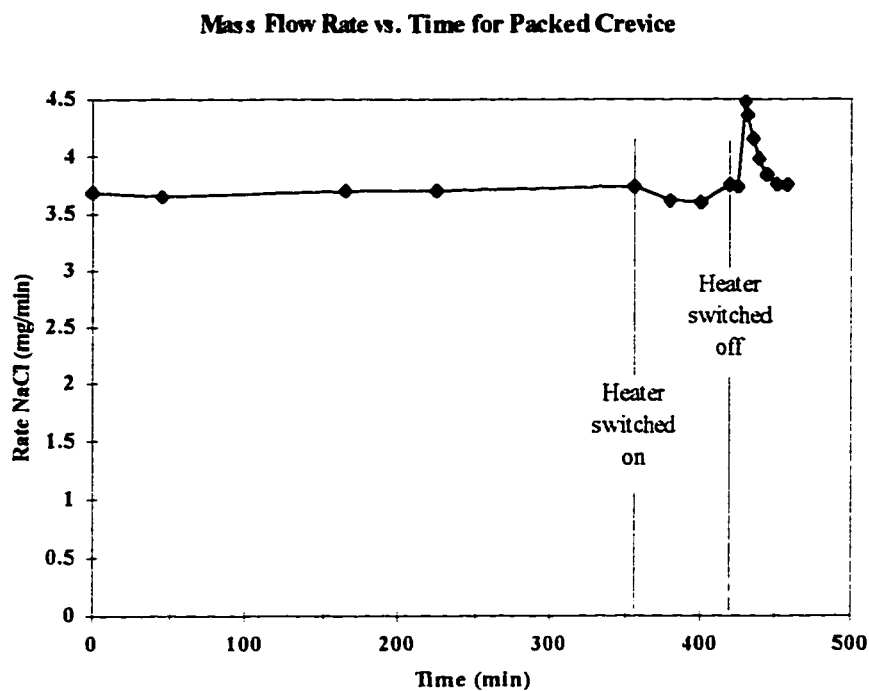


Figure 19. Effluent NaCl Mass Flow Rate for packed crevice experiment.

Figure 19 shows the sodium chloride mass flow rate for the packed crevice experiment as measured by the ion chromatograph. The areas under the curve appear nearly equal because everything that had accumulated in the crevice during hide-out diffused out during hide-out return. The accuracy of the profile, however, is suspect due to the lack of data points, especially in the front end of the surge where only a maximum mass flow rate data point exists. Numerical integration of the area under the curve gave a total crevice mass of 10 ± 180 mg. This number is statistically unsound and approximately 40 samples should have been taken in the 26 minutes of hideout return to obtain a statistically significant standard deviation of less than ± 1 mg. Nevertheless, the fact that

the conductivity did return to near its initial value confirms all impurities that hid in the crevice did diffuse out. Furthermore, although there is a large margin of error, Figure 12 shows results that are compatible to those obtained in the similar experimental work performed by Mann and Castle (Figure 3).

The total crevice volume is 0.0359 in^3 , half of it is occupied by the carbon packing. The total NaCl volume in the crevice was $3.016 \times 10^{-4} \text{ in}^3$, only a small fraction of the remaining crevice volume. Further accumulation was not possible because the thermodynamic limit was reached. The NaCl concentration had gone from 120 ppm in the bulk water to approximately 48,000 ppm in the crevice.

Referring to Figure 19, the sodium chloride flow rate was constant until the time the heater power was turned on. Within a few minutes, the sodium chloride flow rate began to drop. It continued to do so until the thermodynamic limit was reached. Due to boiling point elevation of the crevice solution, the concentration process stopped. That limit was reached after approximately 45 minutes of operating the tube heater at 230 watts. Once the maximum concentration is reached in the crevice, a steady-state condition exists, and the salt being introduced into the system will exit the system without loss. This is reflected in a steady rise in concentration until the original concentration is again obtained.

Hide-out return occurred when the central tube heat flux was removed. The species that were hiding out in the crevice were released and began diffusing into the bulk water and out of the autoclave where they were detected by the analytical instrumentation. The surge began only four minutes after removal of the heat flux, and a peak outlet NaCl

mass flow rate of 4.5 mg/min was attained at approximately ten minutes after heat flux removal. The outlet concentration decayed back to the original value twenty-five minutes after the heat flux was removed.

As a secondary note, upon removal of the central tube heater from the autoclave, it was found that the screws that tighten the cage to the tube were severely corroded. These screws came from San Jose State University's Central Shop and were believed to be stainless 316. Once again, however, the difference in conductivity from inlet to outlet was approximately 1 ppm.

CHAPTER 5. CONCLUSIONS AND RECOMMENDATIONS

The goal of this work has been to design, construct, and confirm the operability of a one-liter autoclave flow process equipped with temperature, pressure, and conductivity measurement instrumentation. Furthermore, a data acquisition system was developed to record process data. In order to complete the work, several vendors were contacted, equipment was specified, and the process was built. The next step was to test the operability of the process.

The system was tested for both steady-state operability and for accumulation in a known packed crevice. The test results were exactly as expected. There was no accumulation in the absence of the cage, while accumulation at predictable rates resulted in a packed crevice experiment. Crevice hideout was observed with the introduction of a heat flux across the central tube. Accumulation ceased as an apparent thermodynamic limit was reached after approximately 45 minutes. Hideout return was observed within four minutes of heat flux removal, with a big surge occurring within ten minutes. It is recommended that the conductivity be continuously monitored because the surge does occur at a very rapid rate, and minutes between sampling would give inadequate data.

Although tests were run in the absence of a cage and in a packed crevice, it would be advisable to perform tests without a crevice, but with the cage installed. The cage is an elaborate piece with many parts, and performing such a test would eliminate all possibilities other than crevice accumulation. The best method of sealing off the crevice is

with Teflon o-rings. The system should be run exactly as in a hideout/hideout return case, with the exception of the sealed crevice. Ideally, there would be no accumulation in the cage, but if there were, it could be quantified and an appropriate correction factor could be included in future work.

The system was not run longer than 25 hours at a time. Over a period of a few runs of comparable length, the piping system sprang a leak. The cause appeared to be pitting corrosion caused by the hot chloride solution breaking down the passive film in the stainless steel wall. A deaerating system was installed to combat this corrosion by removing the dissolved oxygen from the feedwater. Other strategies that may help combat pitting corrosion of the walls include regular cleaning. This could be done by flushing the system with clean, cool, deionized water. Also, suspended solids should be filtered out before introduction into the process. The lines should be flushed out and drained when the system is going to be out of use for extended periods of time. Longer tube life can be obtained by using tubing with a thicker wall. The tubing currently being used has been measured to be thinner than that normally used for this type of service. Finally, and most costly, a more corrosion resistant material could be used to minimize corrosion.

The data acquisition system was also tested and proved reliable for the intended purpose. Testing included direct voltage from a DC power supply, and autoclave process measurements. Autoclave tests included verifying water saturation temperatures at known pressures up to 880 psia. Pressures were verified with a highly accurate digital gage. The accuracy of the instrumentation was very high, showing negligible drift or variance. Through the testing it was observed that without insulating the thermocouple heads from

the hot autoclave, inaccurate measurements would result. This is especially the case with the eight thermocouples that are spot welded to the interior wall of the tube.

This data acquisition system required a great deal of work. Recommendations for the future include purchasing a fully integrated data acquisition system if it exists on the market. If this is not the case, making sure that the company that is selling the equipment is fully knowledgeable in their product. It turned out that the original main data acquisition board was not capable of multiplexing on multiple modules. It took almost an entire year to work out this problem because neither the research team nor the software company was aware of this limitation.

NOMENCLATURE

PWR	Pressurized water reactor	MRI	Molar ratio indicator
SG	Steam generator	ppb	Parts per billion
HOR	Hideout return	ppm	Parts per million
IGA	Intergranular attack	O.D.	Outer diameter
IGSCC	Intergranular stress corrosion cracking	BPR	Back pressure regulator
MRC	Molar ratio control	DAQ	Data acquisition
A_c	Heated area, cm^2		
C	Local concentration, mol/cc		
C_o	Bulk water concentration, mol/cc		
D_o	Bulk diffusion coefficient, cm^2/mol		
D_{es}	Liquid phase effective diffusion coefficient, cm^2/sec		
g	Gravitational acceleration, cm/sec^2		
H	Heat transfer coefficient, $\text{cal/cm}^2/\text{sec}/^\circ\text{C}$		
h_{fg}	Latent heat of vaporization, cal/g		
k	Permeability, cm^2		
k_{rl}	Liquid relative permeability, cm^2		
k_{v-l}	Vapor-liquid distribution coefficient		
L	Depth of crevice or deposit, cm		
P	Capillary pressure, N/cm^2		
P_l	Liquid phase pressure, N/cm^2		
P_v	Vapor phase pressure, N/cm^2		
Q	Heat flux, cal/cm^2		
Re_v	Reynolds number		
r_{sg}	SG tube circumference, cm		
S	Liquid phase saturation		
S_e	Effective saturation		
S_r	Reduced saturation		
T_p	SG tube side temperature, $^\circ\text{C}$		
T_s	Pore solution saturation temperature, $^\circ\text{C}$		
t	Time, sec		
v_l	Superficial liquid velocity, cm/sec		
v_v	Superficial vapor velocity, cm/sec		
W_l	Wetted length, cm		
x	Distance, cm		
ε	Porosity		
ρ_l	Liquid density, g/cm^3		
ρ_v	Vapor density, g/cm^3		

ρ_m	Pore solution density, g/cm ³
μ_l	Liquid viscosity, N sec/cm ²
μ_v	Vapor viscosity, N sec/cm ²

REFERENCES

1. Douglas, John, "Solutions for Steam Generators," EPRI Journal, pp. 29-34, May/June 1995.
2. Hermansson, Hans-Peter, Persson, Goran, Reinvall, Anneli, Corrosion Product Particles in Boiling Water Reactor Condensates, Nuclear Technology, v. 103, pages. 101-113, July 1993.
3. Jones, Denny A., Principles and Prevention of Corrosion, Prentice Hall, second edition, New Jersey, 1996.
4. Mann, G.M.W., Castle, R., "Hideout and Return of Chloride Salts in Heated Crevices Prototypic of Support Plates in Steam Generators," EPRI NP-5015, Electric Power Research Institute, January 1987.
5. Millet, Peter, Steam Generator Degradation: Current Mitigation Strategies for Controlling Corrosion," Presented at CNRA/CSNI Workshop on Steam Generator Tube Integrity in Nuclear Power Plants, October/November 1995.
6. Millet, Peter, Fenton, James, "A Modeling Study of Parameters Controlling Local Concentration Processes in Pressurized Water Reactor Steam Generators", Nuclear Technology, pp. 256 - 265, vol. 108, November 1994.
7. Millet, P.J., PhD Dissertation, University of Connecticut, June 1991.

8. Millet, Peter, Fenton, James M., "A Detailed Model of Localized Concentration Processes in Porous Deposits of SG's," Proceedings of the Fifth International Symposium on Environmental Degradation of Materials in Nuclear Power Systems Water Reactors, pp. 745-751, August, 1991.
9. Millet, Peter J., Fenton, James M., "Review of PWR Steam Generator Crevice Impurity Concentration Mechanisms," Proceedings of a conference on Steam Generators and Heat Exchangers, 1990.
10. Riess, R., Millet, Peter, "State of the Art in Nuclear Plant Cycle Chemistry," Presented at the 12th International Conference on the Properties of Water and Steam, September, 1994.
11. PWR Molar Ratio Control Application Guidelines, Volume 1: Summary. EPRI TR-104811-V1, January 1995.